Performance Analysis of PLC Systems with Diversity Combining under Correlated Lognormal Fading and Nakagami Noise

Chadi Abou-Rjeily[1]

[1]Department of Electrical and Computer Engineering, Lebanese American University, Byblos, Lebanon
*chadi.abourjeily@lau.edu.lb

Abstract: In this paper, we evaluate the Bit Error Rate (BER) performance of multichannel Power Line Communication (PLC) systems under lognormal fading and Nakagami-m background noise. The information signal propagates over two parallel but correlated channels while maximum ratio combining (MRC) and equal gain combining (EGC) are implemented at the receiver side. By appropriately approximating the tail of the probability density function of a single Nakagami-m noise term and of the weighted sum of two Nakagami-m noise terms, we derive accurate expressions of the BER. We prove that single-channel and multichannel PLC systems both benefit from an infinite diversity order and that this quantity increases logarithmically with the signal-to-noise ratio. In this case, the advantage of the diversity combining techniques resides in their impact on the average energy of the fading gain; a quantity that we derive analytically by applying the lognormal-sum approximation.

1. Introduction

Power Line Communication (PLC) is attracting significant attention as an emerging technology for high-speed home area networks. This constitutes a simple and cost-effective solution where communications take place over the existing power lines that are initially installed for power supply. The main sources of impairment in PLC systems are related to the noise and channel characteristics.

PLC suffers from two types of noise; namely, the impulsive noise and background noise [1, 2]. The impulsive noise has a short duration with random occurrence and high power spectral density while the stationary background noise includes the colored background noise and narrow-band noise and has root-mean-square amplitudes that vary slowly over time [1, 2]. It is known that the characterization of noise in PLC systems is difficult to accomplish given the high dependence on the network topology, connected electrical appliances, types of electrical loads and external sources of interference. While the Bernoulli-Gaussian and Middleton distributions are often adopted to model impulsive noise [3, 4], long-term measurements of background noise spectrum conducted at laboratory and residential sites suggested that the probability distribution of the time-domain noise amplitudes can be accurately modeled using the Nakagami-m distribution [2]. The Nakagami noise model was adopted in a large number of contributions that targeted the performance analysis of PLC systems. The probability density function (PDF) of the real part of the Nakagami-like background noise was derived in [5] and then used in [6] to evaluate the performance of Binary Phase Shift Keying (BPSK). This type of modulation was also studied in [7, 8, 9] under Nakagami

background noise and in [10] under a mixture of Nakagami background noise and Middleton impulsive noise. Finally, the Bit Error Rate (BER) performance of Frequency Shift Keying (FSK) under Nakagami noise was analyzed in [11, 12, 13].

In addition to noise, channel fading constitutes a critical impairment that severely degrades the performance of PLC systems. The subject of channel modeling is of paramount importance since the validity of all derived results strongly depend on the validity of the adopted channel model. In order to be able to derive unspecific results and draw general conclusions that hold for a variety of PLC network conditions, we opt to base our analysis on the statistical channel modeling approach rather than the site-specific approach. Several PLC channel models have been proposed in the literature and improvements on these models are still in progress; however, a universally valid statistical channel model is still lacking. Among the most widely accepted channel models, the lognormal distribution fits the statistics of the channel gains in several scenarios [14, 15, 16, 17, 18]. In this context, a statistical analysis of indoor single-phase narrow-band PLC channels based on distributed-element transmission line models was carried out in [14] where it was demonstrated that the path amplitudes follow the lognormal distribution. The impact of the network attributes on the parameters of the lognormally distributed first arriving path of multi-path PLC channels was articulated in [15]. Measurements performed over low-voltage and medium-voltage PLC channels in [16, 17, 18] supported the findings pertaining to lognormal statistics. The lognormal model has been applied in numerous recent references that targeted the performance analysis of PLC systems [8, 19, 20, 21, 22]. While [8] targeted the performance of single-channel systems under the Nakagami background noise, [19, 20, 21, 22] tackled the performance under the Bernoulli-Gaussian impulsive noise.

Since fading constitutes a dominant impairment in PLC systems, diversity combining techniques were advised for these systems [19, 20, 23, 24]. In this context, the information-bearing signal propagates over multiple channels and the received signals are combined for the sake of enhancing the fidelity of signal reconstruction. The multiple channels can be formed using combination from the frequency, time and space domains [19, 20]. In the first two cases, the signals are transmitted over different sufficiently-space frequency bands and different times whose difference exceeds the channel coherence time, respectively. In the last case, different cables or paths are used. In indoor PLC networks, 1-phase 3-wire cables mimic a multichannel system where a pair of electrical wires (with a common ground) is converted to a single channel. In this context, two separate channels are available for communications; namely, the phase-to-ground and neutral-to-ground channels [23, 24].

Our work targets the BER performance analysis of PLC systems under lognormal fading and Nakagami-m noise. The cases of single-channel communication and multichannel communication over two correlated channels are considered. In the latter case, the BERs of Equal Gain Combining (EGC) and Maximum Ratio Combining (MRC) are derived and compared. Benchmarking with the existing literature, the performance under Nakagami-m noise was investigated in [5, 6, 7, 8, 9, 10, 11, 12, 13]. The noise PDF was derived in [5] for the case $m < 1$; in this paper, by adopting a different calculation method we prove that this PDF holds for the case $m \geq 1$ as well. While [6, 7, 10, 11, 12, 13] ignore fading, our derivations incorporate lognormal fading. Under Nakagami-m noise, the BER performance of single-channel PLC systems with lognormal fading was studied in [8] where the derived expressions were reported in integral forms. In [8], the lognormal PDF was approximated by a gamma PDF thus affecting the findings pertaining to the achievable diversity order. Finally, while [5, 6, 7, 8, 9, 10, 11, 12, 13] are limited to single-channel systems, our results are extended to two-channel systems as well which induces a non-negligible

level of complexity on the BER derivations. While our work adopts the same lognormal statistical channel model as [19, 20, 21, 22], the considered Nakagami noise model remarkably differentiates the calculation methodology compared to the Bernoulli-Gaussian noise model. In fact, while the PDF of the latter type of noise can be written as a mixture of Gaussian PDFs, the PDF of the Nakagami-like noise involves the more complicated Whittaker function rendering all subsequent derivations completely different from what has been proposed in [19, 20, 21, 22].

The mathematical framework presented in this paper can be summarized as follows. We first evaluate the noise PDF for all values of m and we propose an asymptotic PDF approximation that is useful for deriving the conditional BER in closed-form. At a second time, we derive and analyze the approximate PDF of the weighted sum of two noise terms. After evaluating the noise, the conditional BER is derived where the equivalent EGC and MRC channels are approximated by lognormal channels based on the lognormal-sum approximation. The developed framework is useful in providing an asymptotic analysis capturing the high signal-to-noise ratio (SNR) performance. By deriving the average energy of each combining scheme, we quantify the superiority of MRC with respect to EGC and relate the associated gain to the channel variance and correlation parameters. Finally, the derived expressions explicitly capture the dependence of the system performance on the parameter m that is critical for determining the noise levels.

2. System Model

In this paper, we consider the scenario of communicating over the power lines of low-voltage residential systems in the 1.8-30 MHz frequency band. This covers mainly indoor PLC systems as well as outdoor systems corresponding to the low-voltage part of the power distribution network for relatively short distances.

2.1. General Parameters and Single-Channel Systems

We assume a flat fading channel where the bandwidth of the transmitted signal is smaller than the coherence bandwidth of the PLC channel [5, 6, 7, 8, 9, 10, 11]. For a single-input-single-output (SISO) system, if the BPSK symbol $s \in \{\pm A\}$ is transmitted, then the real part of the signal received at the receiver can be written as:

$$r = \mathfrak{h} h s + v \tag{1}$$

where v stands for the real part of the additive background noise. This term can be written as $v = x\cos\theta$ where the phase θ is uniformly distributed over the interval $[-\pi\ \pi]$ while the envelope x follows a Nakagami-m distribution [2]:

$$f_{\text{Nak},m}(x) = 2\frac{(m/\Omega)^m}{\Gamma(m)} x^{2m-1} \exp\left(-\frac{mx^2}{\Omega}\right)\ ;\ x \geq 0 \tag{2}$$

where $m > 0.5$ is the shaping parameter, Ω is the mean power and $\Gamma(.)$ stands for the Gamma function.

In (1), h models fading that results in random fluctuations of the signal power without affecting the power of the additive noise. $\mathfrak{h} = \pm 1$ with the same probability and is introduced to account for the possible polarity inversion of the signal after propagating over the PLC channel. In this work, we will evaluate the performance of PLC systems under lognormal fading where the PDF of h is

given by:

$$f_{\text{LN},\mu,\sigma}(h) = \frac{1}{\sqrt{2\pi}\sigma h} \exp\left(-\frac{(\ln(h)-\mu)^2}{2\sigma^2}\right) \; ; \; h \geq 0 \tag{3}$$

where μ and σ are the mean and the standard deviation of the normal random variable $\ln(h)$.

2.2. Multichannel PLC Systems

Consider PLC communications over two frequency, time or space correlated channels. A typical example corresponds to the two separate phase-to-ground and neutral-to-ground channels that are available for communication in a 1-phase 3-wire system. The input-output relation over each channel is given by:

$$r_n = \mathfrak{h}_n h_n s + v_n \;\; ; \;\; n = 1, 2 \tag{4}$$

where r_n, h_n, $\mathfrak{h}_n$ and v_n stand for the received signal, channel magnitude, channel polarity and noise along the n-th channel, respectively. We assume that v_1 and v_2 are independent and identically distributed. On the other hand, the channel coefficients h_1 and h_2 are identically distributed but correlated to take into account the potentially analogous effects that the signals propagating over the two channels might experience.

The considered multichannel system must be associated with an appropriate diversity combining technique that combines the signals r_1 and r_2 at the receiver. In this work, we will analyze EGC and MRC. For EGC, the detection is based on the following decision variable:

$$R_{\text{EGC}} = \mathfrak{h}_1 r_1 + \mathfrak{h}_2 r_2 = (h_1 + h_2)\, s + (\mathfrak{h}_1 v_1 + \mathfrak{h}_2 v_2) \tag{5}$$

For MRC, the decision variable is given by:

$$R_{\text{MRC}} = \mathfrak{h}_1 h_1 r_1 + \mathfrak{h}_2 h_2 r_2 = \left(h_1^2 + h_2^2\right) s + (\mathfrak{h}_1 h_1 v_1 + \mathfrak{h}_2 h_2 v_2) \tag{6}$$

3. Noise PDF

3.1. SISO

***Proposition* 1.** The PDF of the Nakagami noise term v in (1) takes the following expression for all values of m exceeding 0.5:

$$f_v(v) = \frac{1}{\sqrt{\pi}\Gamma(m)} \left(\frac{m}{\Omega}\right)^{\frac{m}{2}-\frac{1}{4}} v^{m-\frac{3}{2}} \exp\left(-\frac{mv^2}{2\Omega}\right) W_{\frac{m}{2}-\frac{1}{4},\frac{1}{4}-\frac{m}{2}}\left(\frac{mv^2}{\Omega}\right) \tag{7}$$

where $W_{\lambda,\mu}(z)$ stands for the Whittaker function [25, 9.220].

Proof: The proof is provided in Appendix A.

It is worth noting that the expression in (7) was initially derived in [5] for the case $0.5 < m < 1$. The alternative calculation method proposed in Appendix A shows that this expression holds for the case $m \geq 1$ as well.

We denote by $\phi_v(t) = \mathrm{E}\left[e^{itv}\right]$ the characteristic function (CF) of the random variable (RV) v whose PDF is given in (7) where $\mathrm{E}[.]$ stands for the averaging operation.

Since the Whittaker function does not lend itself to simple analytical evaluation, it is important to approximate the PDF expression in (7) so that tractable results can be reached. The approximation of $f_v(v)$ must be accurate especially at the tail of the noise PDF ($v \gg 1$) so that the derived

expressions provide accurate estimates of the BER for average-to-large values of the SNR. This implies that, in the transform domain, the approximation of $\phi_v(t)$ must be accurate for small values of $|t|$.

In what follows, $\Gamma(\alpha)$ stands for the gamma function and $\Phi(\alpha,\gamma;z)$ stands for the confluent hypergeometric function [25, 9.210].

***Proposition* 2.** The noise PDF and CF can be approximated by the following expressions:

$$f_{V_{\text{SISO}}}(v) \triangleq f_v(v) \approx \frac{K_m}{\sqrt{\pi}\Gamma(m)} \left(\frac{m}{\Omega}\right)^{m-\frac{1}{2}} v^{2m-2} \exp\left(-\frac{mv^2}{\Omega}\right) \;\; ; \;\; v \gg 1 \tag{8}$$

$$\phi_v(t) \approx \frac{K_m \Gamma(m-\frac{1}{2})}{\sqrt{\pi}\Gamma(m)} \Phi\left(m-\frac{1}{2};\frac{1}{2},-\frac{\Omega t^2}{4m}\right) \;\; ; \;\; |t| \ll 1 \tag{9}$$

where K_m is the constant given by:

$$K_m \triangleq \sum_{k=0}^{+\infty} \alpha_{m,k} \frac{\Gamma(m-k-\frac{1}{2})}{\Gamma(m-\frac{1}{2})} \tag{10}$$

with $\alpha_{m,0}=1$ and:

$$\alpha_{m,k} = \frac{1}{k!}\left[\lambda_m^2 - \left(\lambda_m - \frac{1}{2}\right)^2\right] \cdots \left[\lambda_m^2 - \left(\lambda_m - k + \frac{1}{2}\right)^2\right] \tag{11}$$

where $\lambda_m \triangleq \frac{m}{2} - \frac{1}{4}$.

Proof: The proof is provided in Appendix B.

3.2. EGC

In order to evaluate the performance with EGC, we first need to derive the PDF of the noise term $V_{\text{EGC}} \triangleq \mathfrak{h}_1 v_1 + \mathfrak{h}_2 v_2$ in (5). The noise terms v_1 and v_2 are identically distributed according to the PDF in (7) resulting in:

$$\phi_{V_{\text{EGC}}}(t) = \phi_v(\mathfrak{h}_1 t)\phi_v(\mathfrak{h}_2 t) = \phi_v^2(t) \tag{12}$$

where the second equality follows since, from (7), $f_v(v)$ is a real and even function implying that $\phi_v(t)$ (its Fourier transform) is a real and even function as well. Therefore, the multiplication of t by ± 1 will not change the result.

Replacing (9) in (12) results in:

$$\phi_{V_{\text{EGC}}}(t) \approx \left[\frac{K_m \Gamma(m-\frac{1}{2})}{\sqrt{\pi}\Gamma(m)}\right]^2 \Phi^2\left(m-\frac{1}{2},\frac{1}{2};-\frac{\Omega t^2}{4m}\right) \tag{13}$$

showing that the CF of V_{EGC} is proportional to the square of a confluent hypergeometric function which, evidently, renders all subsequent manipulations very hard to accomplish. Consequently, additional approximations are mandatory.

We propose the following approximation that turns out to be a key relation for reaching the results reported in this work:

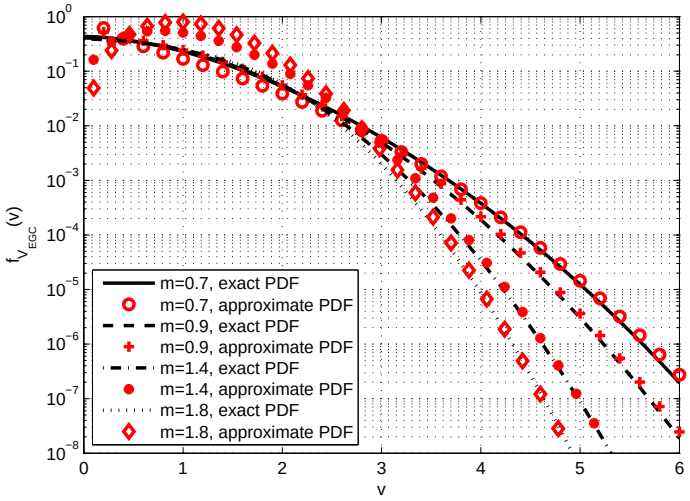

Fig. 1. *Approximate PDFs of noise after EGC.*

***Proposition* 3.** The following approximation holds:

$$\Phi^2(m-\frac{1}{2},\frac{1}{2};z)\approx\Phi(m-\frac{1}{2},\frac{1}{2};2z) \tag{14}$$

where the accuracy of the approximation increases for values of m that are close to 1.

Proof: From the series representation in [25, 9.210.1], it can be observed that $\Phi(m-\frac{1}{2},\frac{1}{2};2z)=1+(2m-1)[2z]+\frac{(2m-1)(2m+1)}{3}\frac{[2z]^2}{2}+\cdots$ while $\Phi^2(m-\frac{1}{2},\frac{1}{2};z)=1+(2m-1)[2z]+\frac{(2m-1)(4m-1)}{3}\frac{[2z]^2}{2}+\cdots$. Consequently, these expressions are close to each other for small values of $|z|$. In this context, the approximation in (14) becomes extremely accurate when $(2m+1)$ is close to $(4m-1)$ and, hence, for values of m that are close to 1.

Replacing (14) in (13):

$$\phi_{V_{\text{EGC}}}(t)\approx\left[\frac{K_m\Gamma(m-\frac{1}{2})}{\sqrt{\pi}\Gamma(m)}\right]^2\Phi\left(m-\frac{1}{2},\frac{1}{2};-\frac{(2\Omega)t^2}{4m}\right) \tag{15}$$

Applying the inverse Fourier transform of (15) using [26, 1.4.14] results in:

$$f_{V_{\text{EGC}}}(v)\approx\left[\frac{K_m\Gamma(m-\frac{1}{2})}{\sqrt{\pi}\Gamma(m)}\right]^2\frac{1}{\Gamma(m-\frac{1}{2})}\left(\frac{m}{2\Omega}\right)^{m-\frac{1}{2}}v^{2m-2}\exp\left(-\frac{mv^2}{2\Omega}\right) \tag{16}$$

The expression in (16) is compared with the exact PDF in Fig. 1 where the results are plotted on a semi-logarithmic scale to better highlight the variations for small values of $f_{V_{\text{EGC}}}(v)$. Results show that the approximate PDF in (16) is very close to the exact PDF for large values of v while the approximation is not very accurate for small values of v. Since our work targets a diversity order analysis, the large SNR regime is considered and, consequently, mainly large noise values potentially yield the majority of the error events. Therefore, in general, any proposed approximation needs to be accurate for large values of v in order to yield accurate asymptotic BERs. In particular, the proposed approximation in (16) meets this target where Fig. 1 shows that the approximate and exact PDFs are barely distinguishable for large values of v (especially given that a

semi-logarithmic scale was considered). In this context, the discrepancy between the two PDFs for small values of v does not affect the accuracy of the BER results presented in this paper.

3.3. MRC

From (6), the noise term is $V_{\text{MRC}} = \mathfrak{h}_1 h_1 v_1 + \mathfrak{h}_2 h_2 v_2$ and its CF is $\phi_{V_{\text{MRC}}}(t) = \phi_v(\mathfrak{h}_1 h_1 t)\phi_v(\mathfrak{h}_2 h_2 t) = \phi_v(h_1 t)\phi_v(h_2 t)$ since $\phi_v(t)$ is an even function. From (9), this results in:

$$\phi_{V_{\text{MRC}}}(t) \approx \left[\frac{K_m \Gamma(m-\frac{1}{2})}{\sqrt{\pi}\Gamma(m)}\right]^2 \prod_{n=1}^{2} \Phi\left(m-\frac{1}{2},\frac{1}{2};-\frac{\Omega h_n^2 t^2}{4m}\right) \tag{17}$$

In a way similar to (14), we introduce the following approximation:

$$\Phi(m-\frac{1}{2},\frac{1}{2};az)\Phi(m-\frac{1}{2},\frac{1}{2};bz) \approx \Phi(m-\frac{1}{2},\frac{1}{2};(a+b)z) \tag{18}$$

where this approximation is extremely close for $m \approx 1$. The proof of (18) is very similar to the proof of (14) and, hence, will be omitted.

Therefore, from (17) and (18):

$$\phi_{V_{\text{MRC}}}(t) \approx \left[\frac{K_m \Gamma(m-\frac{1}{2})}{\sqrt{\pi}\Gamma(m)}\right]^2 \Phi\left(m-\frac{1}{2},\frac{1}{2};-\frac{(h_1^2+h_2^2)\Omega t^2}{4m}\right) \tag{19}$$

Inverting (19) results in:

$$f_{V_{\text{MRC}}}(v) \approx \left[\frac{K_m \Gamma(m-\frac{1}{2})}{\sqrt{\pi}\Gamma(m)}\right]^2 \frac{1}{\Gamma(m-\frac{1}{2})}\left(\frac{m}{(h_1^2+h_2^2)\Omega}\right)^{m-\frac{1}{2}} v^{2m-2}\exp\left(-\frac{mv^2}{(h_1^2+h_2^2)\Omega}\right) \tag{20}$$

4. Conditional BER

***Proposition* 4.** The conditional BERs of SISO, EGC and MRC take the following closed-form expressions:

$$P_{e|h}^{(\text{SISO})} = K'_{m,1}\Gamma\left(m-\frac{1}{2},\frac{mh^2A^2}{\Omega}\right) \tag{21}$$

$$P_{e|\mathbf{h}}^{(\text{EGC})} = K'_{m,2}\Gamma\left(m-\frac{1}{2},\frac{m\left(h_1+h_2\right)^2A^2}{2\Omega}\right) \tag{22}$$

$$P_{e|\mathbf{h}}^{(\text{MRC})} = K'_{m,2}\Gamma\left(m-\frac{1}{2},\frac{m\left(h_1^2+h_2^2\right)^2A^2}{\left(h_1^2+h_2^2\right)\Omega}\right) \tag{23}$$

where $\Gamma(.,.)$ stands for the upper incomplete gamma function and:

$$K'_{m,M} \triangleq \frac{1}{2}\left[\frac{K_m\Gamma(m-\frac{1}{2})}{\sqrt{\pi}\Gamma(m)}\right]^M \frac{1}{\Gamma(m-\frac{1}{2})} \;\;;\;\; M=1,2 \tag{24}$$

Proof: Denote by R the decision variable with $R = r$ in (1) for SISO, $R = R_{\text{EGC}}$ in (5) for EGC and $R = R_{\text{MRC}}$ in (6) for MRC.

The noise PDFs $f_{V_{\text{SISO}}}(v)$, $f_{V_{\text{EGC}}}(v)$ and $f_{V_{\text{MRC}}}(v)$ in (8), (16) and (20) all manifest an even symmetry around the origin. Consequently, the Maximum-Likelihood (ML) decision rule is given by $R \underset{-A}{\overset{+A}{\gtrless}} 0$. Consequently, the BER conditioned on the channel state vector $\mathbf{h} \triangleq [h_1 \;\; h_2]$ is given by:

$$P_{e|\mathbf{h}} = \text{Pr}(s=A)\text{Pr}(R<0|s=A) + \text{Pr}(s=-A)\text{Pr}(R>0|s=-A) \tag{25}$$

which reduces to $P_{e|h}^{(\text{SISO})} = \int_{hA}^{+\infty} f_{V_{\text{SISO}}}(v)\text{d}v$ for SISO, $P_{e|\mathbf{h}}^{(\text{EGC})} = \int_{(h_1+h_2)A}^{+\infty} f_{V_{\text{EGC}}}(v)\text{d}v$ for EGC and $P_{e|\mathbf{h}}^{(\text{MRC})} = \int_{\left(h_1^2+h_2^2\right)A}^{+\infty} f_{V_{\text{MRC}}}(v)\text{d}v$ for MRC where these expressions follow from the symmetry of the noise PDFs. Replacing the PDFs in (8), (16) and (20) in the corresponding integrals and performing the change of variable $x = v^2$ results in the solutions given in (21)-(23) following from [25, 3.381.3].

The considered systems manifest comparable conditional BER expressions as can be observed from (21), (22) and (23). In this context, it is useful to combine these equations in one generic equation as follows:

$$P_{e|\mathbf{h}} = K'_{m,M}\Gamma\left(m - \frac{1}{2}, \frac{m\mathcal{H}A^2}{\Omega}\right) \tag{26}$$

where $M = 1$ (resp. $M = 2$) and $\mathbf{h} = h$ (resp. $\mathbf{h} = [h_1 \;\; h_2]$) for single-channel (resp. multichannel) systems.

The RV $\mathcal{H}$ takes the following values:

$$\mathcal{H} = \begin{cases} \mathcal{H}_{\text{SISO}} \triangleq h^2, & \text{SISO;} \\ \mathcal{H}_{\text{EGC}} \triangleq \frac{(h_1+h_2)^2}{2} = \frac{h_{\text{EGC}}^2}{2}, & \text{EGC;} \\ \mathcal{H}_{\text{MRC}} \triangleq h_1^2 + h_2^2 = h_{\text{MRC}}, & \text{MRC.} \end{cases} \tag{27}$$

5. Average BER and Diversity Orders

5.1. Average BER

We first prove that the RV $\mathcal{H}$ in (27) follows the lognormal distribution in the SISO case while it can be approximated by the lognormal distribution in the cases of EGC and MRC.

5.1.1. SISO: For SISO systems, since h follows the lognormal distribution with parameters μ and σ, then $\mathcal{H}_{\text{SISO}} = h^2$ will also be lognormally distributed with the following parameters:

$$\sigma_{\text{SISO}} = 2\sigma \;\; ; \;\; \mu_{\text{SISO}} = 2\mu \tag{28}$$

5.1.2. EGC:

***Proposition* 5.** In the case of EGC, $\mathcal{H} = \mathcal{H}_{\text{EGC}}$ can be approximated by a lognormal distribution with the following parameters:

$$\sigma_{\text{EGC}}^2 = 4\ln\left(\frac{(1+\rho)e^{\sigma^2} + (1-\rho)}{2}\right) \tag{29}$$

$$\mu_{\text{EGC}} = 2\mu + \sigma^2 + \ln\left(\frac{4}{(1+\rho)e^{\sigma^2} + (1-\rho)}\right) \tag{30}$$

Proof: The RV $h_{\text{EGC}} = h_1 + h_2$ corresponds to the sum of two correlated lognormal RVs. Even though no closed-form expressions for such sum exist in the literature, yet it is well known that the sum of lognormal RVs can be approximated by a lognormal distribution [27, 28]. Consequently, $h_{\text{EGC}} = h_1 + h_2$ will roughly follow a lognormal distribution resulting in a lognormally distributed RV $\mathcal{H}_{\text{EGC}}$ whose parameters will be denoted by μ_{EGC} and σ_{EGC}. These parameters can be determined by numerous methods from which we will apply the Wilkinson's method [27]. In this case, matching the first two moments of $(2\mathcal{H}_{\text{EGC}})^{\frac{1}{2}}$ to the first two moments of $h_1 + h_2$ results in the following equations:

$$e^{\frac{1}{2}\mu_{\text{EGC}} + \frac{1}{2}\ln 2 + \frac{1}{8}\sigma^2_{\text{EGC}}} = 2e^{\mu + \frac{1}{2}\sigma^2} \tag{31}$$

$$e^{\mu_{\text{EGC}} + \ln 2 + \frac{1}{2}\sigma^2_{\text{EGC}}} = 2e^{2\mu + 2\sigma^2} + 2\text{E}[h_1 h_2] \tag{32}$$

On the other hand, the correlation coefficient ρ between h_1 and h_2 is defined as: $\rho = \frac{\text{E}[h_1 h_2] - \text{E}[h_1]\text{E}[h_2]}{\sqrt{\text{var}[h_1]\text{var}[h_2]}}$ where var$[X]$ stands for the variance of the RV X. Replacing $\text{E}[h_1] = \text{E}[h_2] = e^{\mu + \frac{1}{2}\sigma^2}$ and var$[h_1] =$ var$[h_2] = (e^{\sigma^2} - 1)e^{2\mu + \sigma^2}$ results in:

$$\text{E}[h_1 h_2] = e^{2\mu + \sigma^2}[\rho(e^{\sigma^2} - 1) + 1] \tag{33}$$

Replacing (33) in (32) and solving (31)-(32) results in the expressions given in (29)-(30).

5.1.3. MRC:

***Proposition* 6.** In the case of MRC, $\mathcal{H} = \mathcal{H}_{\text{MRC}}$ can be approximated by a lognormal distribution with the following parameters:

$$\sigma^2_{\text{MRC}} = \ln\left(\frac{[\rho(e^{\sigma^2} - 1) + 1]^4 + e^{4\sigma^2}}{2}\right) \tag{34}$$

$$\mu_{\text{MRC}} = 2\mu + 2\sigma^2 + \frac{1}{2}\ln\left(\frac{8}{[\rho(e^{\sigma^2} - 1) + 1]^4 + e^{4\sigma^2}}\right) \tag{35}$$

Proof: The RVs h_1^2 and h_2^2 are lognormally distributed (with parameters 2μ and 2σ), and hence $\mathcal{H}_{\text{MRC}} = h_1^2 + h_2^2$ can be approximated by a lognormal distribution as well. The parameters $(\mu_{\text{MRC}}, \sigma_{\text{MRC}})$ can be obtained by solving:

$$e^{\mu_{\text{MRC}} + \frac{1}{2}\sigma^2_{\text{MRC}}} = 2e^{2\mu + 2\sigma^2} \tag{36}$$

$$e^{2\mu_{\text{MRC}} + 2\sigma^2_{\text{MRC}}} = 2e^{4\mu + 8\sigma^2} + 2\text{E}[h_1^2 h_2^2] \tag{37}$$

In Appendix C, we prove that:

$$\text{E}[h_1^2 h_2^2] = e^{4\mu + 4\sigma^2}\left[\rho(e^{\sigma^2} - 1) + 1\right]^4 \tag{38}$$

Replacing (38) in (37) and solving (36)-(37) results in the expressions given in (34)-(35).

5.1.4. Unified Average BER Expression: As a conclusion, the RV $\mathcal{H}$ in (27) follows the lognormal distribution for all considered systems. Integrating (26) with respect to a lognormal PDF results in the following general expression of the average BER under lognormal fading:

$$P_e = K'_{m,M} \int_0^{+\infty} \Gamma\left(m - \frac{1}{2}, \frac{mA^2}{\Omega} h\right) f_{\text{LN},a,b}(h) \mathrm{d}h \tag{39}$$

where the lognormal PDF is given in (3). The parameters (a, b) depend on the specific system and are given by $(\mu_{\text{SISO}}, \sigma_{\text{SISO}})$, $(\mu_{\text{EGC}}, \sigma_{\text{EGC}})$ and $(\mu_{\text{MRC}}, \sigma_{\text{MRC}})$ in (28), (29)-(30) and (34)-(35) for SISO, EGC and MRC, respectively.

Following from the complexity of the lognormal PDF, it is not possible to obtain a closed-form solution for the integral in (39). Consequently, this integral will be evaluated numerically. Nevertheless, in the following subsection, we will prove that (39) is extremely useful for evaluating the diversity orders under lognormal fading.

5.2. Diversity Orders

***Proposition* 7.** Integrals of the form

$$\mathcal{I} = \int_0^{+\infty} \Gamma\left(s, \frac{mA^2}{\Omega} h\right) \frac{1}{h} e^{-\frac{(\ln(h)-a)^2}{2b^2}} \mathrm{d}h \tag{40}$$

behave asymptotically as $\lim_{d\to+\infty} \left(\frac{mA^2}{\Omega}\right)^{-d}$ where d increases logarithmically with the SNR $\frac{A^2}{\Omega}$.

Proof: The proof is provided in Appendix D.

It is worth noting that the SNR-dependent slope is specific to lognormal fading and differs substantially from what is observed in the case of Rayleigh fading that is often encountered in wireless systems. In fact, for Rayleigh channels, the BER behaves asymptotically as $\left(\frac{mA^2}{\Omega}\right)^{-d}$ where d is a constant and, consequently, the steepness of the BER curve tends to a constant value for large SNRs. On the other hand, for lognormal channels, d becomes a function of the SNR and the steepness of the BER curve will never tend to a constant. In this context, the steepness incessantly increases reaching infinity at infinite SNRs. These findings under Nakagami noise are coherent with the results obtained under Gaussian noise where infinite diversity orders were reported for lognormal fading [29, 30, 31].

The implication of proposition 7 is that when a system has an average BER that is proportional to the integral in (40), then this system will profit from an infinite diversity order. Given that the BERs of the considered SISO, EGC and MRC systems all originate from (39) where simply the values of a and b change from one system to another, then we can conclude that an infinite diversity order can be achieved by all of these systems. In this context, even the single-channel system will profit from an infinite diversity order and the fading-combatting diversity techniques that can not but increase the diversity gain will evidently achieve an infinite diversity order as well.

Even though the diversity techniques can not further boost the diversity order (that is already infinite); however, this should not put in question their usefulness under lognormal fading. In fact, proposition 7 shows that the power d increases logarithmically with the SNR and, hence, the infinite diversity orders would not be perceived below excessively large SNRs that can not be reached in practice. In this context, an important parameter that captures the severeness of

fading can be the average energy $\mathrm{E}[\mathcal{H}]$[1] where $\mathcal{H}$ is given in (27). In this regard, (26) shows that the instantaneous SNR is proportional to $\mathcal{H}$. From (28), (29)-(30) and (34)-(35), we obtain the following expressions:

$$\mathrm{E}[\mathcal{H}_{\mathrm{SISO}}] = e^{\mu_{\mathrm{SISO}}+\frac{1}{2}\sigma^2_{\mathrm{SISO}}} = e^{2\mu+2\sigma^2} \tag{41}$$

$$\mathrm{E}[\mathcal{H}_{\mathrm{EGC}}] = e^{\mu_{\mathrm{EGC}}+\frac{1}{2}\sigma^2_{\mathrm{EGC}}} = e^{2\mu+2\sigma^2} + e^{2\mu+\sigma^2}[\rho(e^{\sigma^2}-1)+1] \tag{42}$$

$$\mathrm{E}[\mathcal{H}_{\mathrm{MRC}}] = e^{\mu_{\mathrm{MRC}}+\frac{1}{2}\sigma^2_{\mathrm{MRC}}} = 2e^{2\mu+2\sigma^2} \tag{43}$$

From (41) and (42), $\mathrm{E}[\mathcal{H}_{\mathrm{EGC}}]-\mathrm{E}[\mathcal{H}_{\mathrm{SISO}}] = e^{2\mu+\sigma^2}[\rho(e^{\sigma^2}-1)+1] = e^{2\mu+\sigma^2(1+\rho_n)} \geq 0$ where (53) was invoked. Consequently, $\mathrm{E}[\mathcal{H}_{\mathrm{EGC}}] \geq \mathrm{E}[\mathcal{H}_{\mathrm{SISO}}]$. In the same way, from (42) and (43), $\mathrm{E}[\mathcal{H}_{\mathrm{MRC}}]-\mathrm{E}[\mathcal{H}_{\mathrm{EGC}}] = e^{2\mu+\sigma^2}\left[e^{\sigma^2}-e^{\sigma^2\rho_n}\right]$. Since $-1 \leq \rho_n \leq 1$, then $\sigma^2 \geq \sigma^2\rho_n$ implying that $\mathrm{E}[\mathcal{H}_{\mathrm{MRC}}] - \mathrm{E}[\mathcal{H}_{\mathrm{EGC}}] \geq 0$ and $\mathrm{E}[\mathcal{H}_{\mathrm{MRC}}] \geq \mathrm{E}[\mathcal{H}_{\mathrm{EGC}}]$. As a conclusion, $\mathrm{E}[\mathcal{H}_{\mathrm{MRC}}] \geq \mathrm{E}[\mathcal{H}_{\mathrm{EGC}}] \geq \mathrm{E}[\mathcal{H}_{\mathrm{SISO}}]$ reflecting the reduction in the fading levels that results from deploying the diversity techniques. Moreover, the first inequality demonstrates the superiority of MRC with respect to EGC for all values of μ and σ where:

$$\frac{\mathrm{E}[\mathcal{H}_{\mathrm{MRC}}]}{\mathrm{E}[\mathcal{H}_{\mathrm{EGC}}]} = \frac{2}{1+e^{-\sigma^2(1-\rho_n)}} \geq 1 \tag{44}$$

The ratio in (44) increases with σ showing that the superiority of MRC manifests especially under strong fading conditions. For small values of σ, this ratio is approximately 1 showing that MRC and EGC will result in comparable performance levels. Finally, $\mathrm{E}[\mathcal{H}_{\mathrm{MRC}}] = 2\mathrm{E}[\mathcal{H}_{\mathrm{SISO}}]$ for all values of μ, σ and ρ.

6. Numerical Results

The parameter σ depends on the communication environment and is often expressed in dB: $\sigma_{\mathrm{dB}} = (10/\ln(10))\,\sigma$ [32]. As in [32], we consider values of σ_{dB} that are equal to 2 dB and 3 dB. We also set $\mu = -\sigma^2$ so that $\mathrm{E}[\mathcal{H}_{\mathrm{SISO}}] = 1$ resulting in a unit energy SISO fading channel.

6.1. Uncorrelated Channels

Figures 2 and 3 show the performance under lognormal fading for $m = 1.8$ where we first consider the case of uncorrelated channel; that is, $\rho = 0$. Fig. 2 shows the performance for $\sigma_{\mathrm{dB}} = 2$ dB while Fig. 3 shows the performance for $\sigma_{\mathrm{dB}} = 3$ dB. Results show the high accuracy of the derived BER expressions where these expressions are extremely close to the exact BERs over the entire SNR range. In fact, in Fig. 2 and Fig. 3, the exact and approximate BERs are barely distinguishable for SNRs exceeding 0 dB and 3 dB, respectively. Moreover, the accuracy of the derived BER expressions is enhanced when σ_{dB} decreases.

Results in figures 2 and 3 highlight the performance gains offered by the diversity combining techniques. Even though the slopes of the curves are not converging to fixed values (infinite diversity orders), yet the diversity techniques result in significant performance gains in the order of 2.8 dB and 3.7 dB for $\sigma_{\mathrm{dB}} = 2$ and $\sigma_{\mathrm{dB}} = 3$ at a BER of 10^{-3}, respectively, showing the usefulness of the diversity techniques especially under severe fading conditions. It happened in this simulation setup that the diversity systems with $\sigma_{\mathrm{dB}} = 3$ (in Fig. 3) result in comparable BERs to SISO systems with $\sigma_{\mathrm{dB}} = 2$ (in Fig. 2) and, hence, the impairment that results from the increased number

[1] Note that $\mathcal{H}$ depends on the square of the path gains and, hence, the energy is given by $\mathrm{E}[\mathcal{H}]$ and not by $\mathrm{E}[\mathcal{H}^2]$.

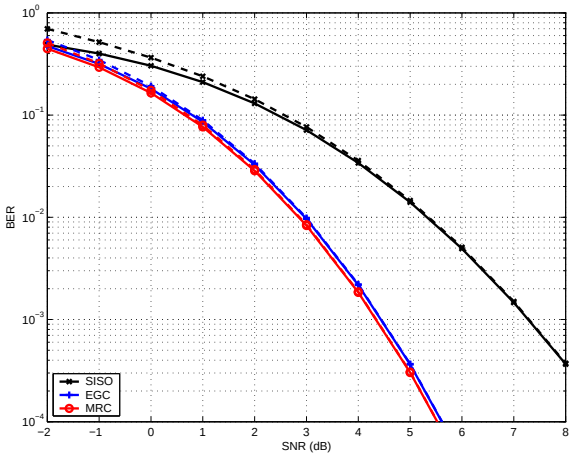

Fig. 2. *BER under uncorrelated lognormal fading for $m = 1.8$ and $\sigma_{dB} = 2$ dB. The solid and dashed lines correspond to the exact and approximate BERs, respectively.*

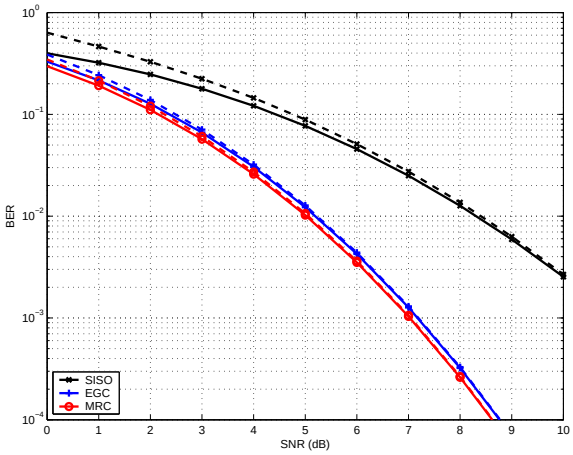

Fig. 3. *BER under uncorrelated lognormal fading for $m = 1.8$ and $\sigma_{dB} = 3$ dB. The solid and dashed lines correspond to the exact and approximate BERs, respectively.*

of branches extending from the main line (that increases σ) can be combatted by deploying the diversity techniques.

Figures 2 and 3 show that EGC and MRC exhibit comparable BERs in coherence with (42)-(43) since the considered values of σ are relatively small. This shows that the implementation of the complex MRC solution (that requires full channel state information (CSI) at the receiver) is not justified since the simple EGC solution (that requires the signs of the path gains only) results in approximately the same performance level. As predicted by our mathematical analysis, the performance gap between MRC and EGC increases with σ; this gap is equal to 0.0835 dB and 0.148 dB for $\sigma_{\text{dB}} = 2$ and $\sigma_{\text{dB}} = 3$, respectively.

6.2. Correlated Channels

Similar results are reported in figures 4 and 5 that highlight the impact of channel correlation on the achievable performance levels for $m = 0.7$. Fig. 4 shows the performance with MRC for

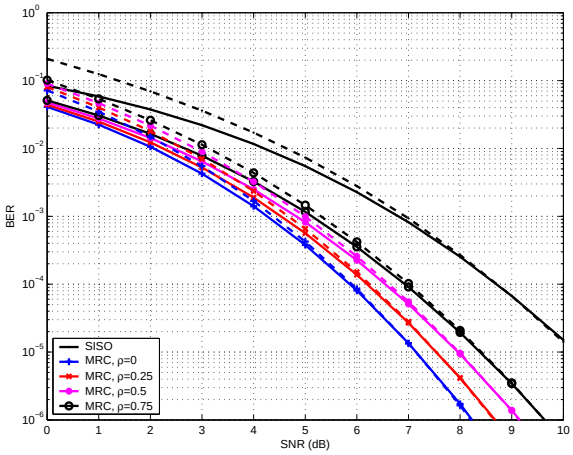

Fig. 4. *BER under correlated lognormal fading with MRC for $m = 0.7$ and $\sigma_{dB} = 2$ dB. The solid and dashed lines correspond to the exact and approximate BERs, respectively.*

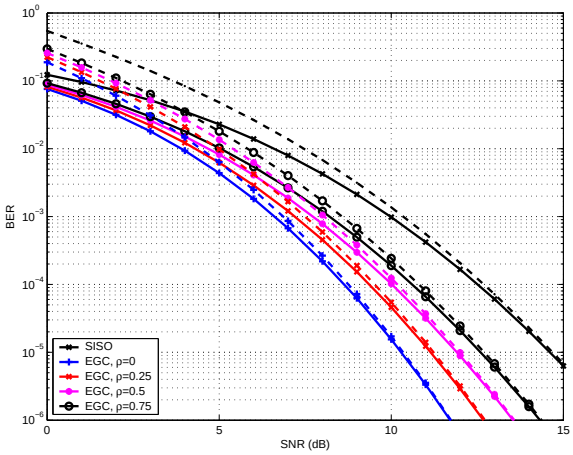

Fig. 5. *BER under correlated lognormal fading with EGC for $m = 0.7$ and $\sigma_{dB} = 3$ dB. The solid and dashed lines correspond to the exact and approximate BERs, respectively.*

$\sigma_{\text{dB}} = 2$ dB while Fig. 5 shows the performance with EGC for $\sigma_{\text{dB}} = 3$ dB. Results highlight the accuracy of the derived expressions in predicting the BER performance with correlated channels especially for average-to-large values of the SNR. It is worth noting that the accuracy declines for large values of ρ since the lognormal sum approximation is less accurate in this case. Evidently, this correlation has no impact on the accuracy of the derived noise PDFs with EGC and MRC.

As predicted by (29)-(30) and (34)-(35), the performance of EGC and MRC deteriorates with increased channel correlation since σ_{EGC} and σ_{MRC} are increasing functions of ρ while μ_{EGC} and μ_{MRC} decrease with ρ. The effect of channel correlation is more prominent for large values of σ as expected since both (33) and (38) are increasing functions of σ. For example, in Fig. 5, for $\sigma_{\text{dB}} = 3$ at a BER of 10^{-4}, performance losses of 0.75 dB and 1.4 dB are incurred (compared to the case of independent channels) for $\rho = 0.25$ and $\rho = 0.5$, respectively.

7. Conclusion

We derived novel BER expressions that offer clear and intuitive insights on the performance of SISO, EGC and MRC systems under lognormal fading and Nakagami noise. The presented analytical framework contributes to a better understanding of the properties of the Nakagami-m noise and its distinctiveness from the Gaussian noise where the following novel findings were reached. (i): The diversity orders of all considered systems were proven to be equal to infinity at asymptotic SNRs. (ii): These diversity orders increase logarithmically with the SNR. (iii): It was proven analytically that the average energy of the equivalent path gain decreases from MRC to EGC and SISO.

A. Exact Noise PDF

The noise term can be written as $v = xy$ where $y = \cos\theta$. Given that θ is uniformly distributed over $[-\pi\ \pi]$, then it can be proven through direct calculations that the PDF of y is:

$$f(y) = \frac{1}{\pi\sqrt{1-y^2}}\ \ ;\quad -1 < y < 1 \tag{45}$$

Following from the relation $v = xy$ and from the independence between x and y [5], the PDF of v can be related to the PDFs $f_X(x)$ and $f_Y(y)$ (of x and y, respectively) by:

$$f(v) = \int_{-\infty}^{+\infty} f_X(x) f_Y(v/x) \frac{1}{|x|} \mathrm{d}x \tag{46}$$

Given that $f_X(x)$ in (2) is defined for $x \geq 0$ and $f_Y(v/x)$ in (45) is defined for $-1 < \frac{v}{x} < 1$, then (46) can be written as:

$$f(v) = 2\frac{(m/\Omega)^m}{\pi\Gamma(m)} \int_{|v|}^{+\infty} x^{2m-1} e^{-\frac{mx^2}{\Omega}} \frac{1}{\sqrt{x^2 - v^2}} \mathrm{d}x \tag{47}$$

Performing the change of variable $t = x^2$ in (47) results in:

$$f(v) = \frac{(m/\Omega)^m}{\pi\Gamma(m)} \int_{v^2}^{+\infty} t^{m-1} \left(t - v^2\right)^{-\frac{1}{2}} e^{-\frac{mt}{\Omega}} \mathrm{d}t \tag{48}$$

(48) can be solved using [25, 3.384.3] where the conditions for which this solution holds are always satisfied: $v^2 > 0$ and $\frac{m}{\Omega} > 0$. Accordingly, (48) simplifies to (7). Note that the only condition on m for which (7) holds is $\frac{m}{\Omega} > 0$ which is satisfied for all positive values of m.

B. Approximate Noise PDF

Following from [25, 9.227] that provides an asymptotic representation of the function $W_{\lambda,\mu}(z)$ for large values of $|z|$, (7) can be approximated by the following expression:

$$f_v(v) \approx \frac{1}{\sqrt{\pi}\Gamma(m)} \sum_{k=0}^{+\infty} \alpha_{m,k} \left(\frac{m}{\Omega}\right)^{m-k-\frac{1}{2}} v^{2m-2k-2} e^{-\frac{mv^2}{\Omega}} \tag{49}$$

where the constant $\alpha_{m,k}$ is defined in (11).

Following from [26, 1.4.14] that provides the Fourier transform of a function having the form $v^a e^{-bv^2}$ and after some straightforward manipulations, the CF associated with the approximation in (49) can be written under the following form:

$$\phi_v(t) \approx \frac{\Gamma(m-\frac{1}{2})}{\sqrt{\pi}\Gamma(m)}\Phi\left(m-\frac{1}{2},\frac{1}{2};-\frac{\Omega t^2}{4m}\right)\sum_{k=0}^{+\infty}\alpha_{m,k}\frac{\Gamma(m-k-\frac{1}{2})}{\Gamma(m-\frac{1}{2})}\frac{\Phi\left(m-k-\frac{1}{2},\frac{1}{2};-\frac{\Omega t^2}{4m}\right)}{\Phi\left(m-\frac{1}{2},\frac{1}{2};-\frac{\Omega t^2}{4m}\right)} \tag{50}$$

From the series representation of $\Phi(\alpha,\gamma;z)$ in [25, 9.210.1]:

$$\frac{\Phi\left(m-k-1/2,1/2;-\Omega t^2/4m\right)}{\Phi\left(m-1/2,1/2;-\Omega t^2/4m\right)} = 1+\frac{k\Omega}{2m}t^2+\cdots\approx 1 \;\;;\;\; |t|\ll 1 \tag{51}$$

Replacing (51) in (50) results in the CF expression given in (9). Applying the inverse Fourier transform of this CF using [26, 1.4.14] results in the PDF expression provided in (8).

C. $\mathbf{E}[h_1^2 h_2^2]$

In this appendix, we will express $\mathrm{E}[h_1^2h_2^2]$ in terms of the parameters μ, σ and ρ. We write h_1 and h_2 as $h_1=e^{X_1}$ and $h_2=e^{X_2}$ where X_1 and X_2 are correlated normal RVs with mean μ and standard deviation σ and whose correlation coefficient will be denoted by ρ_n. The RV X_1+X_2 is normally distributed with mean 2μ and variance $2\sigma^2(1+\rho_n)$ resulting in:

$$\mathcal{M}_{X_1+X_2}(t) = e^{2\mu t+\sigma^2(1+\rho_n)t^2} \tag{52}$$

where $\mathcal{M}_X(t)=\mathrm{E}[e^{tX}]$ stands for the moment generating function of the RV X.

Consequently, from (52), $\mathrm{E}[h_1h_2]=\mathrm{E}[e^{X_1+X_2}]=\mathcal{M}_{X_1+X_2}(1)=e^{2\mu+\sigma^2(1+\rho_n)}$. Comparing this equation with (33) results in:

$$e^{\sigma^2\rho_n} = \rho(e^{\sigma^2}-1)+1 \tag{53}$$

On the other hand, $\mathrm{E}[h_1^2h_2^2]=\mathrm{E}[e^{2(X_1+X_2)}]=\mathcal{M}_{X_1+X_2}(2)=e^{4\mu+4\sigma^2(1+\rho_n)}$. Replacing $e^{\sigma^2\rho_n}$ by its value from (53) results in the expression given in (38).

D. Diversity Order

Performing the change of variable $x=\ln\left(\frac{mA^2}{\Omega}h\right)$, (40) can be written as:

$$\mathcal{I} = \int_{-\infty}^{+\infty}\Gamma(s,e^x)e^{-\frac{\left[x-\ln\left(\frac{mA^2}{\Omega}e^a\right)\right]^2}{2b^2}}\mathrm{d}x \tag{54}$$

Approximating $\Gamma(s,z)$ by $z^{s-1}e^{-z}$ for large values of $|z|$ results in [33]:

$$\mathcal{I} = \int_{-\infty}^{+\infty}e^{(s-1)x}e^{-e^x}e^{-\frac{\left[x-\ln\left(\frac{mA^2}{\Omega}e^a\right)\right]^2}{2b^2}}\mathrm{d}x \tag{55}$$

From [32], the function e^{-e^x} can be approximated by the weighted sum of K Gaussian functions: $e^{-e^x} \approx \sum_{k=1}^{K} r_k \exp\left(-\left(\frac{x-u_k}{v_k}\right)^2\right)$ where r_k, u_k and v_k are constants. Using this approximation, (55) can be written under the following form:

$$\mathcal{I} = \sum_{k=1}^{K} r_k e^{-C_k} \int_{-\infty}^{+\infty} e^{-A_k x^2 + B_k x} \mathrm{d}x \tag{56}$$

where $A_k = \frac{1}{v_k^2} + \frac{1}{2b^2}$ is a constant while B_k and C_k depend on the SNR:

$$B_k = \frac{2u_k}{v_k^2} + \frac{1}{b^2} \ln\left(\frac{mA^2}{\Omega} e^a\right) + (s-1) \tag{57}$$

$$C_k = \frac{u_k^2}{v_k^2} + \frac{1}{2b^2} \left[\ln\left(\frac{mA^2}{\Omega} e^a\right)\right]^2 \tag{58}$$

Equation (56) can be written under the following form:

$$\mathcal{I} = \sum_{k=1}^{K} r_k e^{-C_k + \frac{B_k^2}{4A_k}} \int_{-\infty}^{+\infty} e^{-\frac{\left(x - B_k/2A_k\right)^2}{2\left(1/\sqrt{2A_k}\right)^2}} \mathrm{d}x \tag{59}$$

The integral in (59) is equal to $\sqrt{2\pi}\frac{1}{\sqrt{2A_k}}$ following from the fact that the area under the Gaussian PDF is equal to 1. Consequently:

$$\mathcal{I} = \sum_{k=1}^{K} \sqrt{\frac{\pi}{A_k}} r_k e^{-C_k + \frac{B_k^2}{4A_k}} \tag{60}$$

Replacing A_k, B_k and C_k by their values, (60) can be written under the following form:

$$\mathcal{I} = \sum_{k=1}^{K} \sqrt{\frac{\pi}{A_k}} r_k e^{-\left(D_k + E_k \ln\left(\frac{mA^2}{\Omega} e^a\right) + F_k \left[\ln\left(\frac{mA^2}{\Omega} e^a\right)\right]^2\right)} \tag{61}$$

where $D_k = \frac{u_k^2}{v_k^2} - \frac{1}{4A_k}\left[\frac{2u_k}{v_k^2} + s - 1\right]^2$ and $E_k = -\frac{1}{2A_k b^2}\left[\frac{2u_k}{v_k^2} + s - 1\right]$ are two constants while $F_k = \frac{1}{v_k^2 + 2b^2}$ is a positive constant.

Finally, (61) can be written as:

$$\mathcal{I} = \sum_{k=1}^{K} \sqrt{\frac{\pi}{A_k}} r_k e^{-D_k} \left(\frac{mA^2}{\Omega} e^a\right)^{-E_k - F_k \ln\left(\frac{mA^2}{\Omega} e^a\right)} \tag{62}$$

which behaves asymptotically as:

$$\left(\frac{mA^2}{\Omega} e^a\right)^{-\min\{F_1, \ldots, F_K\} \ln\left(\frac{mA^2}{\Omega} e^a\right)} \tag{63}$$

showing that the diversity order $d = \min_k\{F_k\} \ln\left(\frac{mA^2}{\Omega} e^a\right)$ is infinite for asymptotically large values of the SNR A^2/Ω. Moreover, d increases logarithmically with the SNR completing the proof of proposition 1.

E. References

[1] M. Zimmermann and K. Dostert, "Analysis and modeling of impulsive noise in broad-band powerline communications," *IEEE Trans. Electromagn. Compat.*, vol. 44, no. 1, pp. 249–258, Feb. 2002.

[2] H. Meng, Y. Guan, and S. Chen, "Modeling and analysis of noise effects on broadband power line communications," *IEEE Trans. Power Delivery*, vol. 20, no. 2, pp. 630–637, April 2005.

[3] Y. H. Ma, P. L. So, and E. Gunawan, "Performance analysis of OFDM systems for broadband power line communications under impulsive noise and multipath effects," *IEEE Trans. Power Delivery*, vol. 20, no. 2, pp. 647–682, April 2005.

[4] V. B. Balakirsky and A. J. H. Vinck, "Potential limits on power-line communication over impulsive noise channels," in *Proc. IEEE Int. Symposium on PLC and its Applications*, Mar. 2003, pp. 32–36.

[5] Y. Kim, S. Choi, and H.-M. Oh, "Closed-form expression of Nakagami-like background noise in power-line channel," *IEEE Trans. Power Delivery*, vol. 23, no. 3, pp. 1410–1412, July 2008.

[6] Y. Kim, Y.-H. Kim, H.-M. Oh, and S. Choi, "BER performance of binary transmitted signal for power line communication under Nakagami-like background noise," in *Proc. Int. Conf. on Smart Grids, Green Commun. and IT Energy-aware Technologies*, 2011, pp. 126 – 129.

[7] A. Mathur and M. R. Bhatnagar, "PLC performance analysis assuming BPSK modulation over Nakagami-m additive noise," *IEEE Commun. Lett.*, vol. 18, no. 6, pp. 909–912, June 2014.

[8] A. Mathur, M. R. Bhatnagar, and B. Panigrahi, "Performance evaluation of PLC with log-normal channel gain over Nakagami-m additive background noise," in *Proc. IEEE Int. Conf. on Personal, Indoor and Mobile Radio Commun.*, 2015, pp. 824–829.

[9] A. Mathur, M. R. Bhatnagar, and B. K. Panigrahi, "PLC performance analysis over Rayleigh fading channel under Nakagami-m additive noise," *IEEE Commun. Lett.*, vol. 18, no. 12, pp. 2101–2104, Dec. 2014.

[10] ——, "Performance evaluation of PLC under the combined effect of background and impulsive noises," *IEEE Commun. Lett.*, vol. 19, no. 7, pp. 1117–1120, July 2015.

[11] A. Chandra, A. Gupta, D. Mallick, and A. K. Mishra, "Performance of BFSK over a PLC channel corrupted with background Nakagami noise," in *Proc. IEEE Int. Conf. on Commun. Systems*, 2010, pp. 730–734.

[12] A. Chandra and R. Hazarika, "A comparative study of MFSK and CDMA for power line communication with background Nakagami noise," in *Proc. IEEE Symposium on Indus. Electronics & Applications*, 2010, pp. 195–200.

[13] A. Chattopadhyay, K. Sharma, and A. Chandra, "Error performance of RS coded binary FSK in PLC channels with Nakagami and impulsive noise," in *Proc. IEEE Int. Symposium on PLC and its Applications*, 2014, pp. 184–189.

[14] I. C. Papaleonidopoulos, C. N. Capsalis, C. G. Karagiannopoulos, and N. J. Theodorou, "Statistical analysis and simulation of indoor single-phase low voltage power-line communication channels on the basis of multipath propagation," *IEEE Trans. Consumer Electron.*, vol. 49, no. 1, pp. 89–99, Feb. 2003.

[15] S. Guzelgoz, H. B. Celebi, and H. Arslan, "Statistical characterization of the paths in multipath PLC channels," *IEEE Trans. Power Delivery*, vol. 26, no. 1, pp. 181–187, Jan. 2011.

[16] S. Galli, "A novel approach to the statistical modeling of wireline channels," *IEEE Trans. Commun.*, vol. 59, no. 5, pp. 1332–1345, May 2011.

[17] A. M. Tonello, F. Versolatto, and A. Pittolo, "In-home power line communication channel: Statistical characterization," *IEEE Trans. Commun.*, vol. 62, no. 6, pp. 2096–2106, June 2014.

[18] F. Versolatto and A. M. Tonello, "PLC channel characterization up to 300 MHz: frequency response and line impedance," in *Proc. IEEE Global Telecommun. Conference*, 2012, pp. 3525–3530.

[19] A. Dubey, R. K. Mallik, and R. Schober, "Performance analysis of a power line communication system employing selection combining in correlated log-normal channels and impulsive noise," *IET Commun.*, vol. 8, no. 7, pp. 1072–1082, 2014.

[20] ——, "Performance of a PLC system in impulsive noise with selection combining," in *Proc. IEEE Global Telecommun. Conference*, 2012, pp. 3508–3512.

[21] A. Dubey, D. Sharma, R. K. Mallik, and R. Schober, "Modeling and performance analysis of a PLC system in presence of impulsive noise," in *Proc. IEEE Power and Energy Society General Meeting*, 2015, pp. 1–5.

[22] M. Jani, P. Garg, and A. Bansal, "Performance analysis of a PLC system over log-normal fading channel and impulsive noise," in *Proc. Int. Conf. on Computing and Network Commun.*, 2015, pp. 480–484.

[23] B. Adebisi, S. Ali, and B. Honary, "Space-frequency and space-time-frequency M3FSK for indoor multiwire communications," *IEEE Trans. Power Delivery*, vol. 24, no. 4, pp. 2361–2367, Oct. 2009.

[24] Z. Quan and M. V. Ribeiro, "A low cost STBC-OFDM system with improved reliability for power line communications," in *Proc. IEEE Int. Symposium on PLC and its Applications*, 2011, pp. 261–266.

[25] I. S. Gradshteyn and I. M. Ryzhik, *Table of integrals, series and products*, 6th ed., 2000.

[26] A. Erdelyi, *Tables of Integral Transforms*, vol. I, 1954.

[27] N. C. Beaulieu, A. A. Abu-Dayya, and P. J. Mclane, "Estimating the distribution of a sum of independent lognormal random variables," *IEEE Trans. Commun. Technol.*, vol. 43, pp. 2869–2873, Dec. 1995.

[28] N. C. Beaulieu and Q. Xie, "An optimal lognormal approximation to lognormal sum distributions," *IEEE Trans. Commun. Technol.*, vol. 53, pp. 479–489, Mar. 2004.

[29] M. Safari and M. Uysal, "Cooperative diversity over log-normal fading channels: performance analysis and optimization," *IEEE Trans. Wireless Commun.*, vol. 7, no. 5, pp. 1963 – 1972, May 2008.

[30] C. Abou Rjeily and J. C. Belfiore, "Diversity-multiplexing tradeoff of single-antenna and multi-antenna indoor ultra-wideband channels," in *Proc. IEEE Conf. on UWB*, September 2006, pp. 441 – 446.

[31] H. Nouri, F. Touati and M. Uysal, "Diversity-Multiplexing Tradeoff for Log-Normal Fading Channels," *IEEE Trans. Commun.*, vol. PP, no. 99, pp. 1 – 1, 2016.

[32] A. Dubey, R. K. Mallik, and R. Schober, "Performance analysis of a multi-hop power line communication system over log-normal fading in presence of impulsive noise," *IET Commun.*, vol. 9, no. 1, pp. 1–9, 2015.

[33] [Online]. Available: http://en.wikipedia.org/wiki/Incomplete_gamma_function.